Research Article

Md. Shahid Hasan, Md. Nur Alam*, Md. Fayz-Al-Asad, Noor Muhammad, and Cemil Tunç*

B-spline curve theory: An overview and applications in real life

https://doi.org/10.1515/nleng-2024-0054
received August 13, 2024; accepted October 31, 2024

Abstract: This study commences by delving into B-spline curves, their essential properties, and their practical implementations in the real world. It also examines the role of knot vectors, control points, and de Boor's algorithm in creating an elegant and seamless curve. Beginning with an overview of B-spline curve theory, we delve into the necessary properties that make these curves unique. We explore their local control, smoothness, and versatility, making them well-suited for a wide range of applications. Furthermore, we examine some basic applications of B-spline curves, from designing elegant automotive curves to animating lifelike characters in the entertainment industry, making a significant impact. Utilizing the de Boor algorithm, we intricately shape the contours of everyday essentials by applying a series of control points in combination with a B-spline curve. In addition, we offer valuable insights into the diverse applications of B-spline curves in computer graphics, toy design, the electronics industry, architecture, manufacturing, and various engineering sectors. We highlight their practical utility in manipulating the shape and behavior of the curve, serving as a bridge between theory and application.

*** Corresponding author: Md. Nur Alam,** Department of Mathematics, Pabna University of Science & Technology, Pabna, 6600, Bangladesh, e-mail: nuralam.pstu23@gmail.com, nuralam23@pust.ac.bd
*** Corresponding author: Cemil Tunç,** Department of Mathematics, Faculty of Sciences, Van Yuzuncu Yil University, 65080, Van, Turkey, e-mail: cemtunc@yahoo.com
Md. Shahid Hasan: Department of Mathematics, Pabna University of Science & Technology, Pabna, 6600, Bangladesh, e-mail: shahid.math43@gmail.com
Md. Fayz-Al-Asad: Department of Mathematics, American International University–Bangladesh, Kuratoli, Khilkhet, Dhaka, 1229, Bangladesh, e-mail: fayzmath.buet@gmail.com
Noor Muhammad: School of Mathematics, Sichuan University, Chengdu, Sichuan, 610064, China, e-mail: noormustaffa681@gmail.com, noormuhammad@stu.scu.edu.cn

Keywords: B-spline curves, knot vectors, basis functions, control points, de Boor algorithm, computer-aided design, 3D modeling and graphics

MSC: 65D17, 65D07, 65D05

1 Introduction

Splines, in a broad sense, represent functions formed by combining pieces of smooth functions cohesively and harmoniously. Beyond their theoretical significance, splines find applications in various scientific domains such as geometric representation, signal manipulation, data analysis, visual representation, numerical emulation, and likelihood assessment. Among the diverse family of splines, B-splines (basis splines) distinguish themselves as a cornerstone of modern computational geometry. B-splines offer a sophisticated and efficient framework for the creation of complex curves and surfaces, wielding their influence in domains such as computer-aided geometric design (CAGD) and computer graphics (CG). What sets B-splines apart is their ability to provide local control, allowing for precise adjustments to specific regions of a curve without affecting the entirety of their structure. B-splines are a type of spline basis function that is highly practical because of their numerous beneficial properties. They are specialized instances within splines, which are a generalized form of Bézier curves. B-splines are constructed using instances of an orthonormal basis of recursive functions and can form curves of polynomial nature at specific points called knots. The local support property of B-spline curves greatly benefits real-time applications like interactive design and animation. It allows for efficient updates by ensuring that changes to a control point only affect a localized portion of the curve, rather than requiring a complete recalculation. This feature enhances the responsiveness of interactive design tools, enabling designers to make precise adjustments and see immediate results. In animation, it reduces the computational load by minimizing the need to re-render the entire curve, thus enabling smoother and faster rendering. Additionally, it provides detailed

control over specific parts of animation, allowing for accurate and flexible adjustments. Overall, the local support property facilitates efficient, real-time interaction and precise control in both design and animation tasks. Their ability to handle large data sets with ease makes them indispensable in industries like aerospace, where intricate calculations involving thousands of data points are routine. In summary, B-splines are fundamental tools that contribute significantly to the advancement of precision modeling and design across various engineering and manufacturing domains.

1.1 Background and motivation

The exploration of B-splines traces its origins to the nineteenth century, marked by N. Lobachevsky's contributions [1]. Subsequently, Laplace identified their correlation with the probability density function [2]. They were formulated as convolutions of specific probability distributions, and their relevant properties were extensively explored by Chakalov [3] and Popoviciu [4] in the 1930s. The application of B-splines gained significant traction in 1946 when Isaac Jacob Schoenberg employed them to smooth statistical data, marking the inception of contemporary spline approximation theory [5]. Schoenberg focused on B-splines over uniform knots, whereas the B-splines over non-uniform knots were suggested by his colleague [6]. The significance of B-splines in CAGD saw a substantial boost when de Boor [7], Cox [8], and Mansfield independently unveiled the recursion relation in the same year. The recursion relations were dubbed after de Boor's recursive formula, renowned for its speed and numerical stability. Initially, B-splines were a laborious mathematical method with inconsistent divisions and numerical instability. In 1974, Riesenfeld and Gordon employed de Boor's recursive formula in the parametric B-spline curve, revealing that B-splines naturally generalized the de Casteljau recursive formula used in Bézier curve evaluation [9]. In aerospace engineering, quadratic and cubic B-splines are essential for accurately modeling complex surfaces, such as aircraft wings and fuselages. Additionally, B-splines are integral to computational fluid dynamics simulations, which model the airflow around the aircraft to enhance design effectiveness. Similarly, in civil and structural engineering, B-splines are increasingly utilized to create innovative designs for logistics centers and sports facilities [10,11]. Their versatility across both fields underscores their significance in modern engineering, where the demand for accuracy and esthetic appeal continues to grow. Quadratic B-splines provide smooth transitions and moderate precision, making them suitable for surfaces with moderate curvature and less complexity. They offer a good balance between smoothness and computational efficiency, which is useful for designing various aircraft components. Cubic B-splines, on the other hand, offer a higher degree of smoothness and accuracy. They ensure C^2 continuity, which means the surface transitions smoothly with continuous second derivatives, making them ideal for intricate aerodynamic shapes like wing profiles and fuselage contours. This high level of precision allows for detailed control and optimization of the surface, which is essential for achieving the desired aerodynamic performance and structural integrity. Thus, cubic B-splines are particularly valuable in aerospace engineering for their ability to handle complex geometries with high accuracy and smoothness. Besides B-spline methods have demonstrated significant effectiveness across various boundary value problems, known for their stability and accuracy. The cubic B-spline has been applied to third-order singular equations, such as Emden–Fowler types [12], while quintic polynomial B-splines have been useful for fourth-order equations, including the Kuramoto–Sivashinsky equation [13]. Additionally, quartic B-splines have been applied successfully in both third- and fourth-order singular boundary value problems, enhancing the solution accuracy and efficiency [14,15].

This article aims to provide a widespread understanding of the impact of B-spline curves by exploring their theoretical foundations and real-world applications across various fields. These applications include architectural design, biomedical technology, computer-aided manufacturing (CAM) for precision engineering, and robotics [16–19]. These mathematical constructs have seamlessly integrated themselves into the fabric of modern technology, enabling streamlined and sophisticated design solutions.

Besides, these B-spline curves are pivotal in numerical analysis and CG, with applications ranging from solving differential equations [20–22] to analyzing fractal patterns in retail analytics [23], classifying fractal designs [24], and enhancing online insights through advanced machine learning techniques [25], and so on [26–37]. Mastery of B-spline theory is increasingly essential for innovation in design and engineering, as detailed in works by Rogers, Piegl, and Hoschek [38–41].

1.2 Objectives and outlines of this article

The primary objective of this research is to explore how B-spline functions can be used to create smooth and high-quality curve shapes for real-life applications. By

understanding the theory and practical applications of B-spline curves, this study aims to demonstrate their role in improving the design and appearance of various products and structures in different industries. To summarize, the key features of this study are as follows:

a. Explore the use of B-spline functions to create high-quality smooth curve shapes in practical applications.
b. Understand the theoretical underpinnings and practical implications of B-spline curve theory.
c. Highlight the significance of B-spline curves in enhancing the design and esthetic appeal of products and structures across industries.
d. Emphasize the role of B-spline curves in improving the precision and visual sophistication in contemporary design and engineering practices.

The outlines of the article are organized to facilitate an understanding of B-spline curves and their applications in real life. Section 2 provides an in-depth exploration of B-spline curves and their properties. Section 3 details the construction of B-spline curves. In Section 4, we examine the zero degree, first degree, second degree, and third degree of B-spline curves. Section 5 delves into the practical implementation of B-splines using the de Boor algorithm, illustrating their use in constructing real-world objects. Finally, Section 6 presents a comprehensive conclusion, summarizing the key findings and implications gleaned from this study.

2 B-spline curve and its properties

A B-spline, also known as a basis spline, represents a more flexible form of the Bézier curve. Unlike Bézier curves, which lack local adjustability and where changes to any control point affect the entire curve shape, B-splines offer a solution to this limitation. Researchers developed B-splines to be highly adaptable, with minimal constraints on the degree, smoothness, and domain. Additionally, B-splines ensure C^2-continuity up to a certain degree, making them a versatile and robust tool for curve modeling. The term "basis" in basis spline refers to the fact that they act as basis functions for the spline function space. In simpler terms, B-splines are a way of smoothly connecting points to form a curve. Any spline of degree $(p-1)$ on a given knot sequence can be used to express a unique linear combination of B-splines of the same degree. A $(p-1)$th degree or order p B-spline curve $S(y)$ is defined as

$$S(y) = \sum_{i=1}^{n+1} B_{i,p}(y) C_i, \quad t_{\min} \le y < t_{\max}, \ 2 \le p < n+1, \quad (1)$$

where the weights C_i are position vectors of S defining polygon vertices, which are referred to as control points in the literature because they control the shape of the B-spline curve. The splines $S(y)$ are the points along the curve as a function of parameter y also known as a B-spline curve. $B_{i,p}(y)$ are the normalized basis functions which are polynomials of degree $p-1$. The basis functions are described by order p and a non-decreasing sequence of real numbers called "knot vectors." The knot vectors determine the values of t at which the pieces of curve join, like knots joining bits of a string. It is necessary that $t_i \le t_{i+1}$ (Figure 1).

B-spline curves have several important properties. Some of the key properties are as follows:

- **Local control:** B-spline provides local control over their shape. Changes to one control point or a few control points affect only a localized portion of the curve. This means moving a control point C_i only changes the curve near that control point.
- **Convex hull:** Moving along the curve from one parameter value to another, the curve always lies within the convex hull formed by the control points. That is the curve is enclosed within the convex hull of its control polygon. Moreover, each curve segment resides within the control polygon defined by the control points influencing that specific segment. More specifically, if y belongs to the knot span $[t_i, t_{i+1})$, then $S(y)$ is within the convex hull of the control points $C_{i-p}, C_{i-p+1}, \ldots, C_i$ (Figures 2–4).
- **Continuity:** For a B-spline curve of degree $p \ge 1$, the B-splines belong to the continuity category of C^{p-1}, that is, a third-degree B-spline curve has C^2 continuity (Figures 5 and 6). However, increasing the knot multiplicity r of a knot vector diminishes the continuity of the curve to C^{p-r} at that knot. The smoothness or level of differentiability of a B-spline curve is determined by the number of knot multiplicities. Within each interval $[t_i, t_{i+1})$, a B-spline curve exhibits infinite differentiability.

3 Rules for the construction of the B-spline curve

The B-spline curve, which is a piecewise polynomial curve with the least support, seems to have importance in its ability to intricately craft smooth and adaptable curves and surfaces. A group of control points and a group of basis functions, typically piecewise polynomial functions with

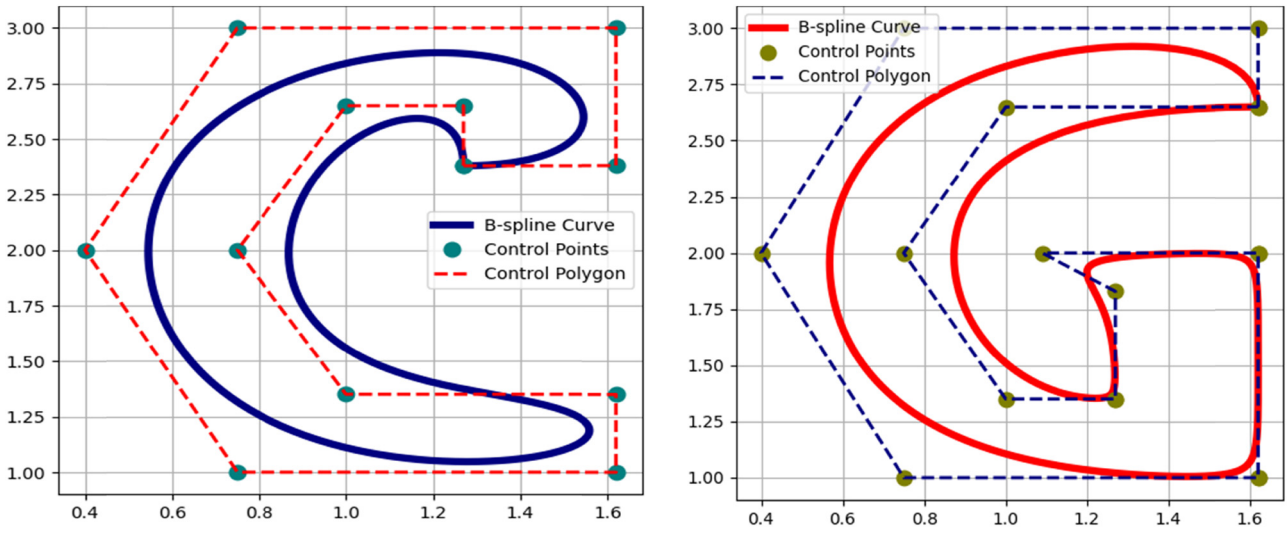

Figure 1: B-spline curve with control points and the defining polygon.

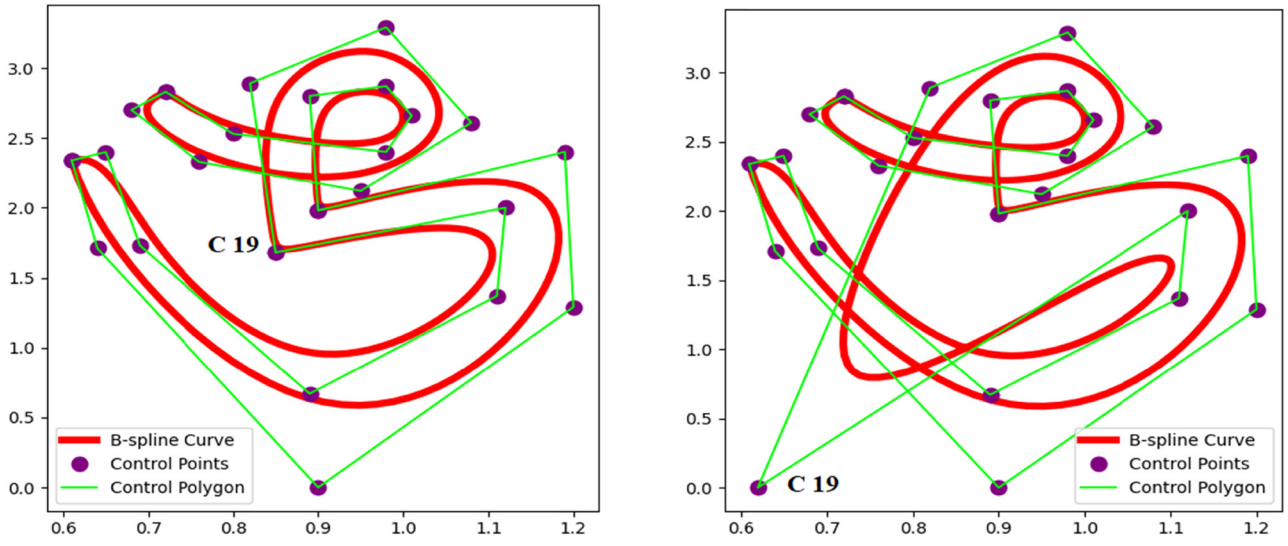

Figure 2: Changing the location of control point C_{19} only affects the curve $S(y)$ within the interval $[t_{19}, t_{23})$.

specific knot sequences, define a B-spline curve. To gain a comprehensive understanding of B-splines and to construct B-spline curves, several things are required. Among them, knot vectors, basis functions, degree or order of basis function, and control points are noticeable.

3.1 Knot vectors

Every B-spine curve consists of segments. The joint points between these segments are known as knots. The knot vector is a sequence of values that determines the parameterization of the B-spline curve or surface. These parameters specify how the domain is divided into segments and how much each basis function affects a certain interval. To achieve desirable curve features, such as smoothness and continuity, the knot vector must be selected carefully. The choice of knot vector must provide enough resolution to approximate the solution of a mathematical problem. The only requirement for a knot vector is that it satisfies the relation, $t_i \leq t_{i+1}$, *i.e.*, it is a monotonically increasing series of real numbers. There are three

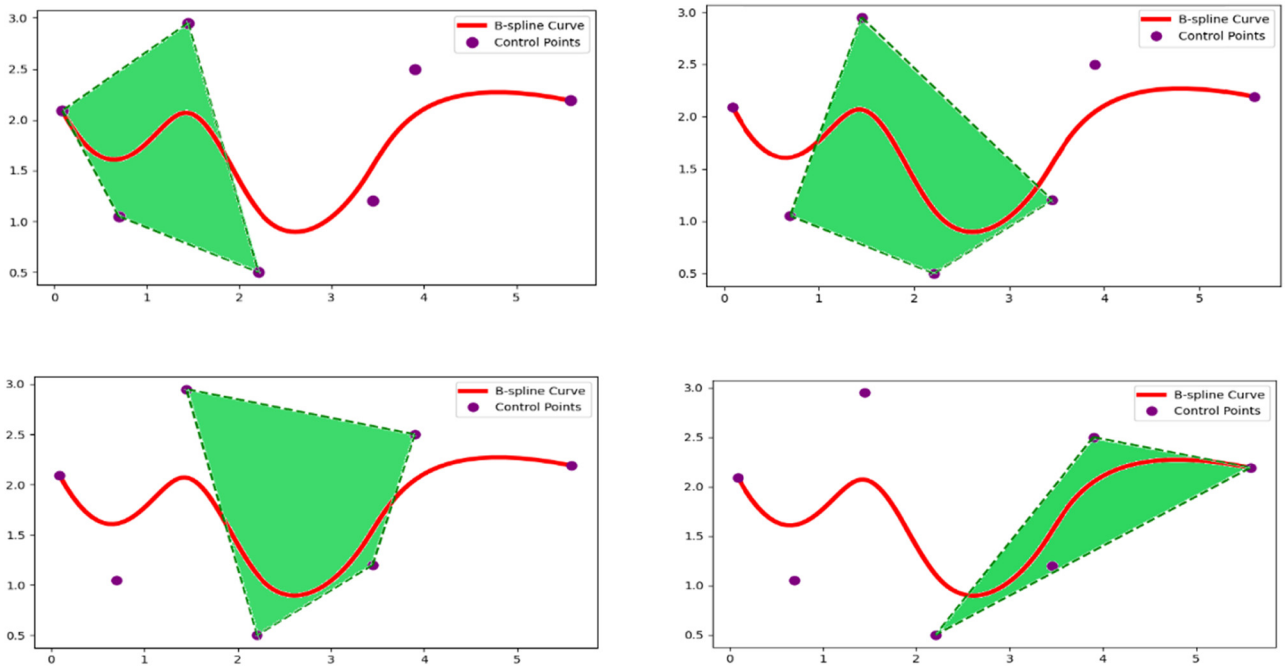

Figure 3: First, second, third, and fourth knot spans are contained in the convex hull of C_0, C_1, C_2, ... ,C_6.

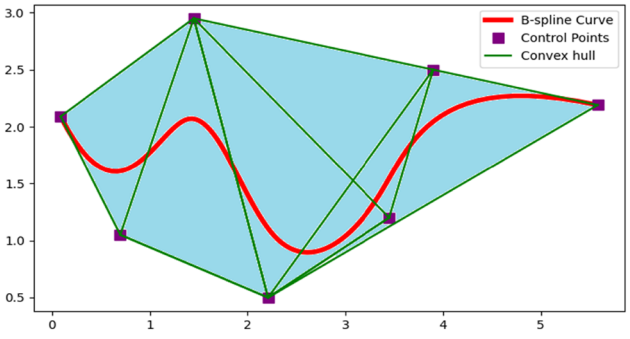

Figure 4: Union of convex hulls yields a tighter B-spline curve boundary.

types of knot vectors such as the uniform knot vector, open uniform knot vector, and non-uniform knot vector.

3.1.1 Uniform knot vector

Uniform knot vectors have individual knot values that are evenly spaced along the parameter domain. These are knot values for which $t_{i+1} - t_i = h$ = constant and $i = 0, 1, 2 ..., \quad n$.

For example, [0 1 2 3 4 5 6], and [−1.4 − 0.3 0.8 1.9 3.0].

Sometimes, knot values are normalized in the range between 0 and 1. An example of this is [0 0.25 0.5 0.75 1].

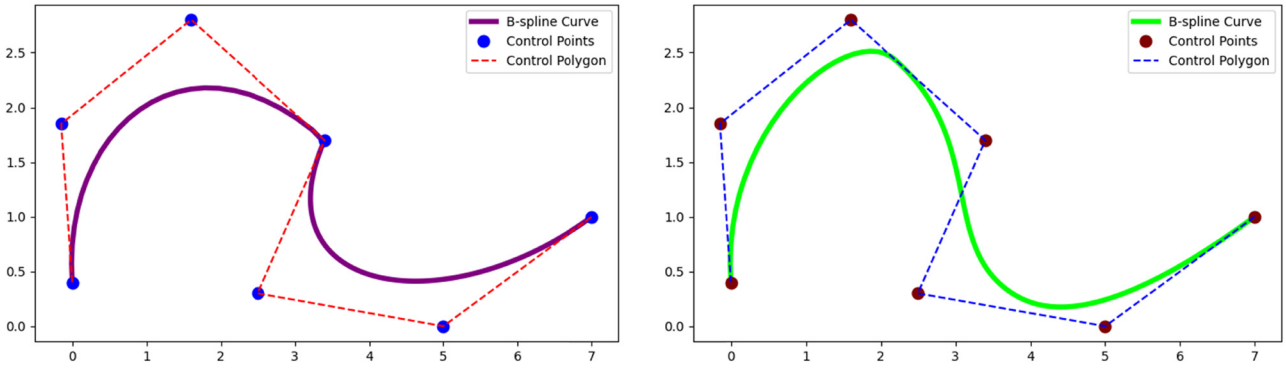

Figure 5: B-spline curve with C^0(left) and C^1 continuous knots (right).

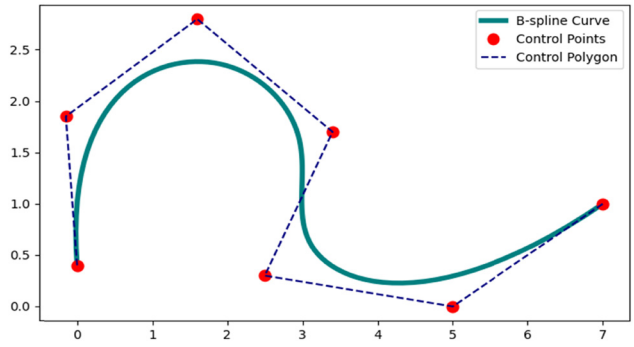

Figure 6: C^2 continuous B-spline curve.

The periodic uniform knot vector arises when the B-spline curve is closed, the spacing between the knot values is fixed, and the knot vector starts at zero and is incremented by 1 to some maximum value.

3.1.2 Open uniform (non-periodic) knot vector

An open uniform knot vector is a type of knot vector that has a multiplicity of knot values at the ends equal to the degree $(p - 1)$ of the B-spline basis function, where the B-spline curve does not form a closed loop, meaning it starts and ends at different points. The pth order B-spline $B_{i,p}(y)$, $i = 0, 1, 2,\ldots,$ n is defined for the parameter $y \in [0, n - p + 2]$. The uniform non-periodic knots t_0 to t_{n+p} of a non-periodic curve are chosen based on the following rule.

$$t_i = \begin{cases} 0, & 0 \le i < p \\ i - p + 1, & p \le i < n \\ n - p + 2, & n < i \le n + p. \end{cases} \tag{2}$$

For example, [0 0 0 0 1 2 3 4 4 4 4], [0.1 0.1 0.1 0.3 0.5 0.5 0.5], and [0 0 0 1 /3 2/3 1 1 1].

In general, the choice of knots according to Eq. (2) is found to provide the following knot structure for open uniform (non-periodic) curves:

$$[\underbrace{0\,0\,0\ldots 0}_{p\text{ knots}}\,1\,2\,3\ldots n-p + 1\,\underbrace{n-p+2\,n-p+2\,n-p+2\ldots n-p+2}_{p\text{ knots}}].$$

The control polygon and spline's endpoints are aligned through the repeated knots, with p knots at the beginning, p at the end, and $n - p + 1$ in between. As a result, any open uniform polygon has $p + (n - p + 1) + p$ or $n + p + 1$ total knots (Figure 7).

3.1.3 Non-uniform knot vectors

Non-uniform knot vectors have varying lengths between consecutive knots and can be unequally spaced with or without multiple internal knots. Some examples of non-uniform knot vectors are

[0 1 1 2 3 3 4 5], [0 0.26 0.44 0.70 1], and [0 0 0 1 1 2 2 2 3 4 4 4].

3.2 Basis functions

After the selection of the knot vector, the B-spline basis function can be calculated. B-spline basis functions $B_{i,p}(y)$ are piecewise-defined polynomial functions that partition the parametric domain t into segments, each associated with a particular control point. They determine how the control points are combined to form the curve, while the control points affect the curve's position and shape. Using the idea of divided difference, the initial

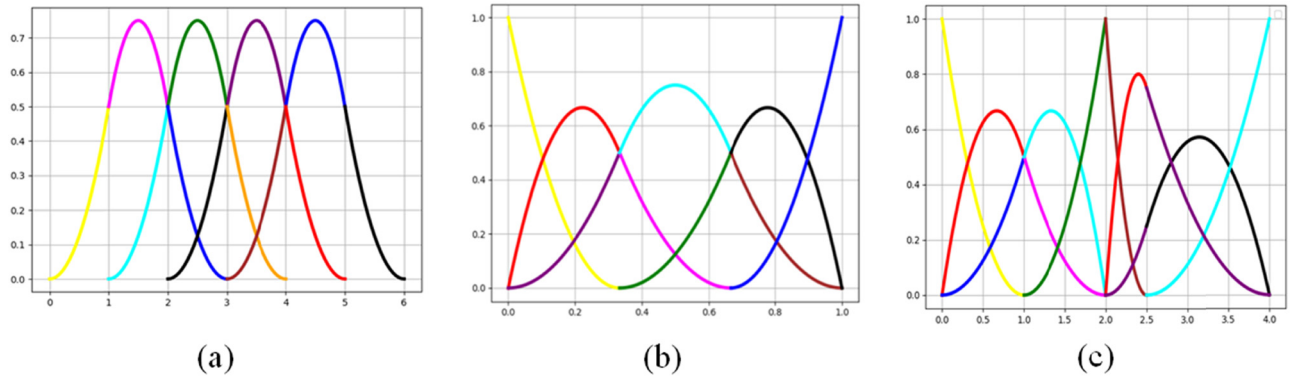

Figure 7: (a) Quadratic B-spline basis functions defined in a uniform knot vector [v] = [0 1 2 3 4 5 6]; (b) quadratic B-spline basis functions defined in an open uniform knot vector [v] = [0 0 0 1/3 2/3 1 1 1]; (c) quadratic B-spline basis functions defined in a non-uniform knot vector [v] = [0 0 0 1 2 2 2.5 4 4 4].

definition of the B-spline basis functions was provided by Schumaker. The de Boor algorithm enhances the efficiency of curve and surface evaluations in computer-aided design (CAD) by providing a stable and numerically efficient method for evaluating B-spline curves and surfaces. Here's how it improves upon traditional methods:

- ✓ **Local control**: The de Boor algorithm utilizes the local properties of B-splines, which means that each point on the curve is influenced by a small number of control points. This local support reduces the number of computations needed for curve evaluation, making it more efficient than methods that require global recalculation.
- ✓ **Numerical stability**: Unlike some traditional polynomial-based methods, the de Boor algorithm avoids numerical instability issues caused by high-degree polynomials. This is achieved by breaking down the curve into lower-degree polynomial segments, which are easier to compute and less prone to round-off errors.
- ✓ **Recursive structure**: The algorithm employs a recursive approach based on the Cox–de Boor recursion formula, which efficiently computes the B-spline basis functions. This recursive computation allows for a systematic reduction of the problem size, further enhancing the computational efficiency.
- ✓ **Handling complex geometries**: In CAD, complex surfaces are often represented using B-spline patches. The de Boor algorithm can handle these efficiently by evaluating points on surfaces using a similar approach, benefiting from the recursive, local, and stable properties of B-splines.

Overall, the de Boor algorithm is specifically designed to leverage the properties of B-splines, making it more efficient than traditional polynomial interpolation methods for curve and surface evaluations in CAD applications. After that, de Boor discovered a recurrence relation in the 1970s [24,25] to determine the higher-degree B-spline basis functions by using Leibnitz's theorem. For a given knot sequence t, ith B-spline basis functions of arbitrary pth degree can be given recursively as follows:

$$B_{i,p}(y) = \frac{y - t_i}{t_{i+p-1} - t_i} B_{i,p-1}(y) + \frac{t_{i+p} - y}{t_{i+p} - t_{i+1}} B_{i+1,p-1}(y), \quad (3)$$

where $t_i \le y < t_{i+p}$ and

$$B_{i,1}(y) = \begin{cases} 1 & \text{if } t_i \le y < t_{i+1} \\ 0 & \text{otherwise,} \end{cases} \quad (4)$$

where $B_{i,p}(y)$ defines an ith B-spline basis function of $p-1$th degree and demonstrates that the basis functions of any degree can be stably interpreted as a linear combination of basis functions of lower degree. The recurrence relation constructs the higher-degree basis functions, starting with the first-degree B-spline. The values of t_i are determined by a prearranged knot vector that satisfies the relationship $t_i \le t_{i+1}$. The basis functions and knot vectors are described using a parameter y, which serves as a coordinate in a parameter space and may or may not align with any of the Cartesian coordinates. Note that in the case of repeated knots in B-spline curves, the curve becomes zero at the end-knots t_i and t_{i+p}, that is, $B_{i,p}(y = t_i) = 0$ and $B_{i,p}(y = t_{i+p}) = 0$. However, in B-splines, the utilization of repeated knots (*i. e.*, $t_i = t_{i+1} = t_{i+2} = \cdots$) is a common practice. Thus, the expression $B_{i,p}(y)$ can take the form 0/0, and in this context we consider 0/0 as equivalent to 0 to incorporate repeated knots. To trace the $p-1$th degree curve, $S(y)$ in Eq. (1), the parameter y varies within the range from 0 to $n - p + 2$. It can be displayed that for any value of the parameter y, the sum of the basis functions $\sum_{i=0}^{n} B_{i,p}(y) = 1$.

Hence, the B-spline curve is contained within the convex hull determined by its control polygon.

We list a few more properties of the basis functions $B_{i,p}(y)$ that are a consequence of the definition as follows:

- Local the support property: $B_{i,p}(y) = 0$ for t outside the interval $[t_i, t_{i+p}]$, where t_i is the i th knot value.
- Normalizing property: $\sum_{i=0}^{n} B_{i,p}(y) = 1$ for $y \in [t_p, t_{n+1}]$.
- Non-negativity property: $\sum_{i=0}^{n} B_{i,p}(y) \ge 0$ for y within the interval $[t_p, t_{n+1}]$.
- Knot multiplicity: knots with multiplicity result in C^p continuity at that knot.
- Continuity at joint: $B_{i,p}(y)$ has continuity C^{p-2} at each knot t_i. C^{p-2} is the derivative degree for $B_{i,p}(y)$ at each t_i equal to $p-2$.

3.3 Control points

Control points in B-spline curves are a set of points that influence the shape and behavior of the curve. These points define the curve's geometry and allow for precise control over its shape mirroring the corners of a defining polygon, which are instrumental in crafting the curve and guiding its overall structure and behavior. They allow for precise customization of B-spline curves, enabling adjustments for smoothness, curvature, and local variations.

Control points and basis functions are intimately connected. The curve or surface at any given parameter value is a linear combination of control points weighted by the basis functions. In the case of B-spline surfaces, control points can also hold information about the tangent and normal directions, which are essential for specifying the orientation of the surface at those points. In this thesis, the Greville Abscissa approach is employed to determine the positions of the control points along the B-spline curve. If we confine the control point's abscissa values to align with the Greville abscissa, it, in turn, imposes constraints on the "X" Cartesian coordinates of the parameter coordinate "y". The formula for calculating these coordinates is as follows:

$$x_i = \frac{1}{p}(t_i + t_{i+1} + t_{i+2} + \ldots + t_{i+p-1}) \text{ for } i = 0, 1, \ldots h - p, \quad (5)$$

where h is the total number of knots in the knot vector and p is the degree of the basis function. Control points play a crucial role in B-spline curves, and they are essential for shaping and controlling the curve. Here are some key applications of control points in B-spline curves as follows:

- Curve shape and positioning: The position of control points directly influences the shape and position of the B-spline curve. Moving control points can be used to adjust the curve's trajectory, create curves with specific features, or reposition the entire curve.
- Smoothness and continuity: Control points govern the degree of smoothness and continuity of the B-spline curve. By adjusting the positions of control points, one can achieve various levels of curve continuity, such as C^0 (position continuity), C^1 (tangent continuity), and C^2 (curvature continuity).
- Local modification: B-spline curves allow for local modifications, which is not the case with some other curve representations. This means that a limited number of control points can be adjusted to change only a portion of the curve without affecting the rest of the curve. This feature makes B-splines particularly useful for interactive design and editing.
- Deformation and animation: B-spline curves are often used in CG and animation. Control points allow animators to deform and reshape characters, objects, or paths by manipulating the positions of control points over time.
- Geometric modeling: B-spline curves are used in CAD and CAM for modeling complex shapes. Control points enable the precise definition and manipulation of these shapes.
- Curved surfaces: B-spline curves are building blocks for creating B-spline surfaces. Control points for B-spline surfaces define not only curves but also entire 2D or 3D surfaces. Control points play a similar role in shaping and controlling the surface as they do in curves.

3.4 Relation between knot vectors and the number of control points

There is a fundamental relationship between the number of knot vectors, control points, and the order of a B-spline curve. Given a knot sequence $[V] = [t_0, t_1, \ldots, t_n]$, there are $n + 1$ knots. When determining the basis functions for a curve of a given order p, there are $n - p$ basis functions. This is a direct outcome of the inductive argument used in generating the basis functions. To define a B-spline using these basis functions, $S(y) = \sum_{i=0}^{n} B_{i,p}(y)C_i$, where $B_{i,p}(y)$ are the basis functions and C_i are the position vectors called the control points. The requirement is that the number of control points, denoted by $m + 1$, should be equivalent to the number of basis functions $n - p$. When constructing B-spline curves, it is important to emphasize that a curve is only defined when the sum of the basis functions equals one. This property ensures that we have a barycentric representation of the points. It is a bookkeeping task to show that the sum of these basis functions equals one within the interval $t_p \le y \le t_{n-p}$. An important observation to make is that we can only define a curve when the order lies within the range $0 \le p \le n/2$.

4 Degrees of B-splines

Consider a non-decreasing knot sequence $t_0, t_1, \ldots, t_{i-1}, t_i, t_{i+1}, \ldots, t_n$ that satisfies $t_{i-1} \le t_i \le t_{i+1}$ for $i = 0, 1, 2, \ldots, n$. The B-spline function of degree p is defined recursively as:

$$B_{i,p}(y) = \frac{y - t_i}{t_{i+p} - t_i} B_{i,p-1}(y) + \frac{t_{i+p+1} - y}{t_{i+p+1} - t_{i+1}} B_{i+1,p-1}(y), \quad y \in (t_i, t_{i+p+1}). \quad (6)$$

In this article, we provide the first degree, second degree, third degree, and fourth degree of the B-spline curve which are provided in the following.

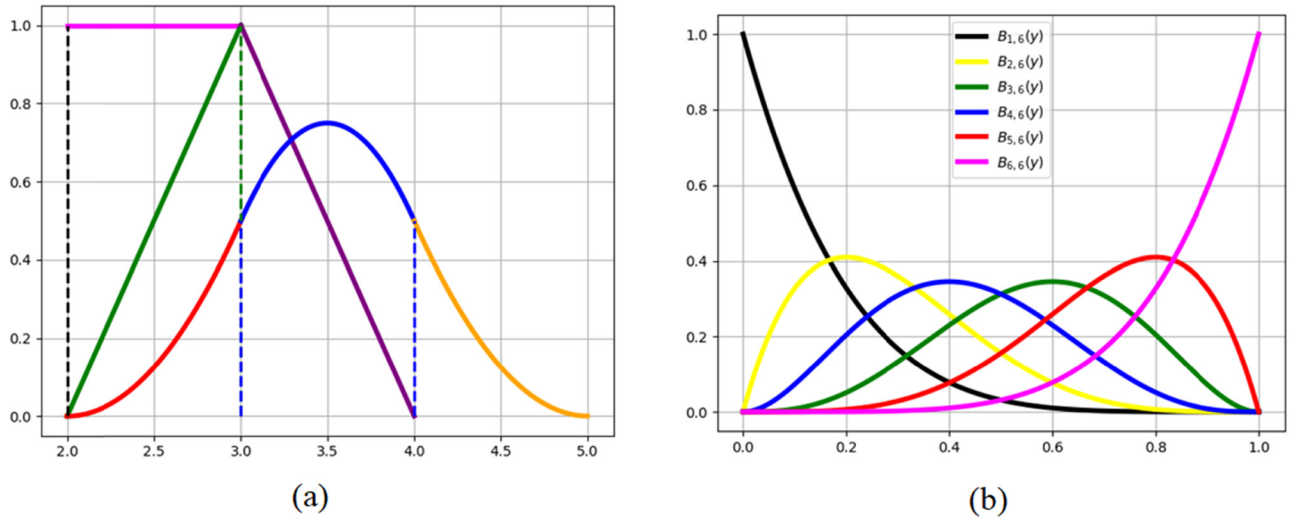

Figure 8: (a) The three lowest basis functions corresponding to a uniform knot structure; (b) basis function for the sixth order B-spline approximation with non-periodic knots.

4.1 Zero-degree B-spline

The zero degree or first-order B-spline is one of the simplest basis functions defined as

$$B_{i,0}(y) = \begin{cases} 1 & \text{if } t_i \le y < t_{i+1} \\ 0 & \text{otherwise.} \end{cases} \tag{7}$$

Thus, for $p = 0$, the basis function is just a step function, which means it is zero at all points except on the semi-open interval $[t_i, t_{i+1})$.

Suppose that the knots are $t_0 = 0$, $t_1 = 1$, and $t_2 = 2$. The basis function of the first order, $B_{0,0}(y) = 1$ in the knot span (0,1), but $B_{0,0}(y) = 0$ elsewhere, $B_{0,0}(y) = 1$ in the knot span (1,2), but $B_{0,0}(y) = 0$ in elsewhere, and so on. Each basis function exhibits a discontinuity at those knots, meaning that they possess C^{-1} continuity, specifically at these knot points. Figure 8 shows the plot of the B-spline basis function of zero degree.

4.2 First-degree B-spline

The first-degree (second-order) B-splines are known as linear B-splines and can be obtained by using the recursion formula (6) with degree $p = 1$ along with the zero-degree B-spline formula (7) as follows:

$$B_{i,1}(y) = \frac{y - t_i}{t_{i+1} - t_i} B_{i,0}(y) + \frac{t_{i+2} - y}{t_{i+2} - t_{i+1}} B_{i+1,0}(y). \tag{8}$$

Substituting the values of

$$B_{i,0}(y) \text{ and } B_{i+1,0}(y),$$

we obtain:

Combining both, we have

$$B_{i,1}(y) = \begin{cases} \dfrac{y - t_i}{t_{i+1} - t_i} & \text{if } t_i \le y < t_{i+1} \\ \dfrac{t_{i+2} - y}{t_{i+2} - t_{i+1}} & \text{if } t_{i+1} \le y < t_{i+2} \\ 0 & \text{otherwise.} \end{cases} \tag{9}$$

To express $B_{i,1}(y)$ explicitly, by setting $t_{i+1} - t_i = h$ and $i = 0, 1, 2, \ldots, n$, we obtain

$$B_{i,1}(y) = \frac{1}{h} \begin{cases} y - t_i & \text{if } t_i \le y < t_{i+1} \\ t_{i+2} - y & \text{if } t_{i+1} \le y < t_{i+2} \\ 0 & \text{otherwise.} \end{cases} \tag{10}$$

The function $B_{i,1}(y) = \frac{1}{h}(y - t_i)$ is in knot span $[t_i, t_{i+1})$, $B_{i,1}(y) = \frac{1}{h}(t_{i+2} - y)$ is in knot span $[t_{i+1}, t_{i+2})$, and $B_{i,1}(y) = 0$ elsewhere. Figure 8 shows that the first-degree B-splines are like a "tent" or "hat," and each of the two consecutive knots are joined and the continuity C^0.

4.3 Second-degree B-spline

The second-degree B-splines or quadratic B-splines can be obtained by using the Cox–de Boor recursion formula (6) and linear B-splines (9) given by:

$$B_{i,2}(y) = \begin{cases} \dfrac{(y - t_i)^2}{(t_{i+2} - t_i)(t_{i+1} - t_i)} & t_i \le y < t_{i+1} \\ \dfrac{(y - t_i)(t_{i+2} - y)}{(t_{i+2} - t_i)(t_{i+2} - t_{i+1})} + \dfrac{(t_{i+3} - y)(y - t_{i+1})}{(t_{i+3} - t_{i+1})(t_{i+2} - t_{i+1})} & t_{i+1} \le y < t_{i+2} \\ \dfrac{(t_{i+3} - y)^2}{(t_{i+3} - t_{i+1})(t_{i+3} - t_{i+2})} & t_{i+2} \le y < t_{i+3} \\ 0 & \text{otherwise.} \end{cases} \tag{11}$$

The explicit formula of Eq. (11) by setting $t_{i+1} - t_i = h$, $i = 0, 1, 2, \ldots, n$. is given by

$$B_{i,2}(y) = \frac{1}{2h^2}\begin{cases} (y - t_i)^2 & t_i \le y < t_{i+1} \\ (y - t_i)(t_{i+2} - y) + (t_{i+3} - y)(y - t_{i+1}) & t_{i+1} \le y < t_{i+2} \\ (t_{i+3} - y)^2 & t_{i+2} \le y < t_{i+3} \\ 0 & \text{otherwise.} \end{cases} \tag{12}$$

The quadratic B-splines $B_{i,2}(y)$ are non-zero on the knot spans $[t_i, t_{i+1})$, $[t_{i+1}, t_{i+2})$, and $[t_{i+2}, t_{i+3})$. Each of the three knot spans contains quadratic polynomials except for those starting from t_{i+3} and beyond. These functions exhibit C^1 continuity at the knots. Figure 8 depicts that the three polynomials are joined to each other smoothly.

4.4 Third-degree B-spline

A third-degree B-spline also known as the cubic B-spline is generated by putting $p = 3$ in Eq. (6) and using the quadratic B-spline Eq. (11), which is given by

$$B_{i,3}(y) = \begin{cases} \dfrac{(y - t_i)^3}{(t_{i+3} - t_i)(t_{i+2} - t_i)(t_{i+1} - t_i)} & t_i \le y < t_{i+1} \\ \dfrac{(y - t_i)^2(t_{i+2} - y)}{(t_{i+3} - t_i)(t_{i+2} - t_i)(t_{i+2} - t_{i+1})} + \dfrac{(y - t_i)(t_{i+3} - y)(y - t_{i+1})}{(t_{i+3} - t_i)(t_{i+3} - t_{i+1})(t_{i+2} - t_{i+1})} + \dfrac{(t_{i+4} - y)(y - t_{i+1})^2}{(t_{i+4} - t_{i+1})(t_{i+3} - t_{i+1})(t_{i+2} - t_{i+1})} & t_{i+1} \le y < t_{i+2} \\ \dfrac{(y - t_i)(t_{i+3} - y)^2}{(t_{i+3} - t_i)(t_{i+3} - t_{i+1})(t_{i+3} - t_{i+2})} + \dfrac{(t_{i+4} - y)(y - t_{i+1})(t_{i+3} - y)}{(t_{i+4} - t_{i+1})(t_{i+3} - t_{i+1})(t_{i+3} - t_{i+2})} + \dfrac{(t_{i+4} - y)^2(y - t_{i+2})}{(t_{i+4} - t_{i+1})(t_{i+4} - t_{i+2})(t_{i+3} - t_{i+2})} & t_{i+2} \le y < t_{i+3} \\ \dfrac{(t_{i+4} - y)^3}{(t_{i+4} - t_{i+1})(t_{i+4} - t_{i+2})(t_{i+4} - t_{i+3})} & t_{i+3} \le y < t_{i+4} \\ 0 & \text{otherwise.} \end{cases} \tag{13}$$

The explicit formula of Eq. (13) by setting $t_{i+1} - t_i = h$, $i = 0, 1, 2, \ldots, n$. is given by

$$B_{i,3}(y) = \frac{1}{6h^3}\begin{cases} (y - t_i)^3 & t_i \le y < t_{i+1} \\ h^3 + 3h^2(y - t_{i+1}) + 3h(y - t_{i+1})^2 - 3(y - t_{i+1})^3 & t_{i+1} \le y < t_{i+2} \\ h^3 + 3h^2(t_{i+3} - y) + 3h(t_{i+3} - y)^2 - 3(t_{i+3} - y)^3 & t_{i+2} \le y < t_{i+3} \\ (t_{i+4} - y)^3 & t_{i+3} \le y < t_{i+4} \\ 0 & \text{otherwise.} \end{cases} \tag{14}$$

From the above cubic B-spline, we see that each knot span has cubic polynomials except for the intervals starting from knots t_{i+4} onward. Figure 9 shows the third-degree (fourth order) B-spline. Each of the polynomials is smoothly connected, ensuring continuity up to the second derivative (C^2 continuity).

5 Utilizing B-spline curves in industrial contexts

In this section, we delve into the diverse industrial applications of B-spline curves, exploring their use cases in various domains. Through the manipulation of control points, knot vectors, degrees of curve, and continuity, we uncover their instrumental role in fields such as manufacturing, engineering design, CG, and more. From the creation of smooth, flexible designs to the precise modeling of complex shapes, B-spline curves have proven indispensable in streamlining industrial processes and enhancing the overall product quality. Enhancing the discussion with details on the impact of B-splines in fields like biomedical engineering and robotics can significantly enrich the practical applications. In biomedical engineering, B-splines are instrumental in 3D imaging, prosthetic design, and tissue modeling, offering precise and adaptable solutions for complex structures. In robotics, they facilitate smoother, more accurate motion control, enabling efficient navigation in dynamic environments. Highlighting these applications emphasizes the versatility and precision of B-splines in cutting-edge, real-world technologies.

5.1 Car modeling

The selection of control points and knot vectors is crucial in determining the accuracy and shape of a B-spline curve. Strategically placed control points ensure the curve accurately represents the car's features, such as edges, curves, and corners. A higher density of control points offers greater flexibility and precision for capturing fine details but can introduce complexity, while too few points may lead to an oversimplified and

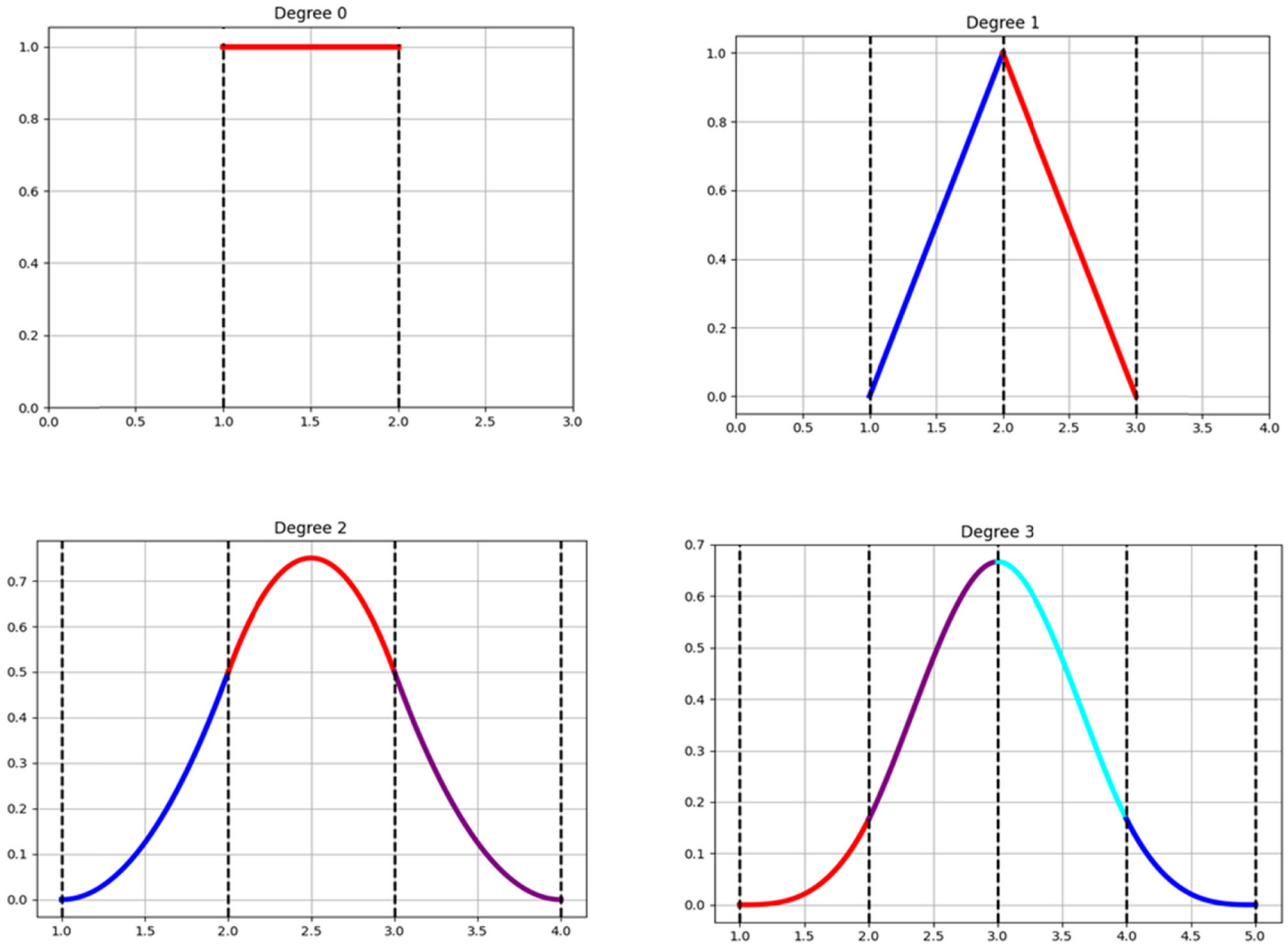

Figure 9: B-spline of varying degrees from 0 to 3 represented with knots (black dashed lines).

less accurate shape. Also, the selection of knot vectors significantly influences the shape of the B-spline curve. Uniform knot vectors create a smooth, evenly distributed curve but may lack precision in capturing sharp features or detailed areas. In contrast, non-uniform knot vectors offer more localized control, allowing the curve to closely follow specific control points and accurately represent sharp features and intricate details by clustering knots where needed.

In order to generate a smooth car-shaped curve, we utilized a second-degree B-spline and non-uniform knot vectors containing 68 knot values. By applying the B-spline curve technique with the de Boor algorithm, we were able to create both the original car shape and a refined, smoother version, as shown in Figure 10.

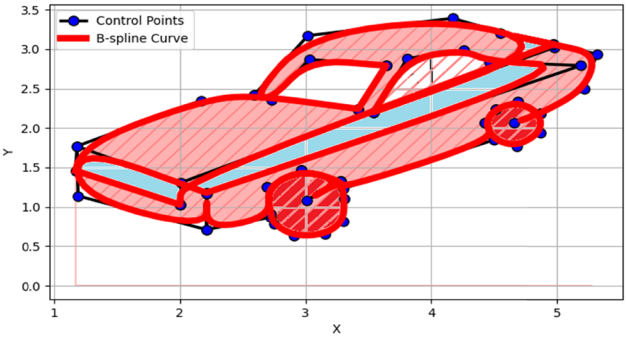

Figure 10: Car modeling using the B-spline curve with control points [1.17, 1.46], [1.18, 1.77], [2.17, 2.35], [2.59, 2.42], [3.42, 2.24], [3.42, 2.24], [3.64, 2.79], [3.64, 2.79], [3.03, 2.87], [2.73, 2.36], [2.59, 2.42], [3.02, 3.17], [4.17, 3.39], [4.98, 3.02], [3.54, 2.20], [3.54, 2.20], [3.81, 2.88], [4.26, 2.99], [4.46, 2.84], [5.19, 2.79], [2.21, 1.18], [2.21, 1.18], [1.18, 1.77], [2.215, 1.169], [2.21, 0.71], [2.72, 0.87], [2.69, 1.25], [2.97, 1.47], [3.28, 1.33], [3.011, 1.084], [3.28, 1.33], [3.31, 1.10], [3.30, 0.82], [3.156, 0.65], [2.91, 0.63], [2.75, 0.78], [2.72, 0.91], [2.69, 1.25], [2.97, 1.47], [3.28, 1.33], [3.302, 1.234], [4.50, 1.85], [4.43, 2.07], [4.51, 2.24], [4.69, 2.33], [4.87, 2.18], [4.87, 1.94], [4.68, 1.77], [4.50, 1.85], [4.43, 2.07], [4.51, 2.24], [4.69, 2.33], [4.87, 2.18], [4.66, 2.07], [4.87, 2.18], [5.22, 2.49], [5.318, 2.937], [4.972, 3.06], [4.55, 3.20], [4.972, 3.06], [4.972, 3.06], [2.01, 1.31], [2.00, 1.03], [2.00, 1.03], and [1.17, 1.46].

5.2 Modeling of the jet aircraft

Adjusting the degree of the B-spline curve has a significant impact on aerodynamic efficiency:

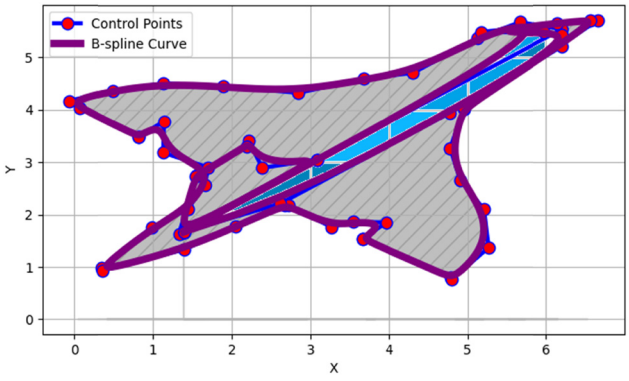

Figure 11: Jet aircraft shape using the B-spline curve with control points [1.39, 1.67], [3.08, 3.05], [3.08, 3.05], [2.39, 2.89], [2.22, 3.40], [2.19, 3.30], [1.55, 2.74], [1.54, 2.73], [1.33, 1.63], [1.39, 1.67], [6.20, 5.54], [5.67, 5.68], [5.12, 5.37], [4.31, 4.71], [3.68, 4.60], [2.85, 4.33], [1.89, 4.45], [1.13, 4.51], [0.49, 4.37], [−0.07, 4.17], [0.07, 4.04], [0.82, 3.49], [0.82, 3.49], [1.14, 3.78], [1.13, 3.18], [1.70, 2.90], [1.66, 2.57], [1.44, 2.10], [0.98, 1.75], [0.34, 0.98], [0.36, 0.93], [1.39, 1.33], [2.05, 1.77], [2.67, 2.18], [2.72, 2.17], [3.27, 1.76], [3.54, 1.86], [3.97, 1.85], [3.66, 1.54], [3.67, 1.53], [4.79, 0.80], [4.80, 0.76], [5.27, 1.37], [5.21, 2.10], [4.91, 2.65], [4.78, 3.27], [4.96, 4.02], [4.96, 4.03], [6.66, 5.71], [6.56, 5.71], [6.14, 5.65], [5.17, 5.49], [5.97, 5.48], [6.20, 5.44], [6.20, 5.21], [4.77, 3.94], [2.62, 2.21], and [1.39, 1.67].

- ✓ Higher-degree B-splines: Provide smoother transitions between segments, reducing the aerodynamic drag and turbulence. They offer greater precision in modeling complex shapes and contours, ensuring that the design closely matches the intended aerodynamic profile. This results in more efficient airflow, improved lift, and reduced drag. Additionally, higher-degree splines allow for better control over surface curvature, enabling fine-tuning to meet specific aerodynamic requirements and optimize the performance.

- ✓ Lower-degree B-splines: May lead to less smooth transitions, creating potential discontinuities or sharp corners that increase the drag and reduce the aerodynamic efficiency. They offer less precision in capturing intricate aerodynamic features and provide limited control over surface curvature, which can constrain the ability to optimize performance characteristics.

In order to generate a smooth jet aircraft-shaped curve, we utilized a fourth-degree B-spline and non-uniform knot vectors containing 63 knot values. By using the de Boor algorithm with B-spline curves, we successfully create both the original jet plane shape and an improved, smoother version, as shown in Figure 11.

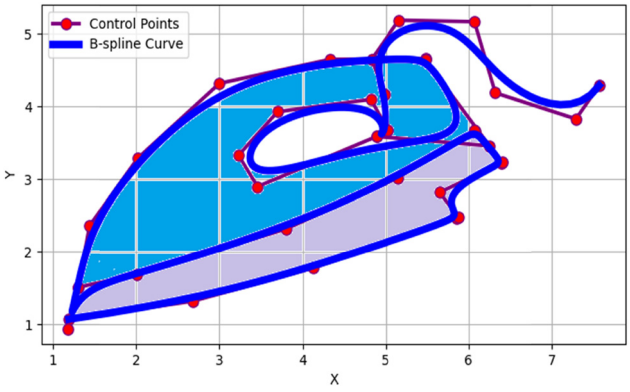

Figure 12: Designing of the electric iron using the B-spline curve with control points [1.19, 1.07], [2.68, 1.32], [4.13, 1.78], [5.86, 2.47], [5.88, 2.48], [5.65, 2.82], [6.39, 3.22], [6.40, 3.23], [6.08, 3.66], [6.07, 3.67], [5.15, 3.02], [3.80, 2.32], [2.01, 1.69], [1.30, 1.51], [1.18, 0.94], [1.30, 1.51], [1.44, 2.36], [2.02, 3.29], [3.00, 4.32], [4.33, 4.65], [5.48, 4.66], [5.48, 4.65], [6.25, 3.46], [4.89, 3.59], [3.46, 2.90], [3.23, 3.33], [3.70, 3.93], [4.82, 4.10], [5.03, 3.67], [4.89, 3.59], [5.03, 3.67], [4.99, 4.17], [4.83, 4.65], [5.16, 5.19], [6.07, 5.17], [6.32, 4.19], [7.29, 3.83], and [7.57, 4.29].

5.3 Electric iron designing

B-spline curves offer key advantages over cubic splines for designing real-world objects like electric irons. They provide greater flexibility and local control, allowing for precise shaping and fine-tuning of specific areas. Besides they ensure smooth transitions and continuity, which is crucial for both esthetics and functionality. Additionally, they can use non-uniform knot vectors for better detail and adaptability and offer improved numerical stability, making them well-suited for complex and accurate designs.

To produce a sleek electric iron-shaped curve, we employed a fourth-degree B-spline along with non-uniform knot vectors comprising 43 knot values. Through the implementation of the de Boor algorithm with B-spline curves, we effectively developed both the initial electric iron shape and a refined, more polished rendition, exemplified in Figure 12.

5.4 Shape of the plastic chair

In the context of creation of the shape of plastic toys and products, B-spline allows designers to shape contours and fine-tune specific areas for optimal comfort and esthetics. This control ensures that the final product is both functional and visually appealing, highlighting the effectiveness of advanced

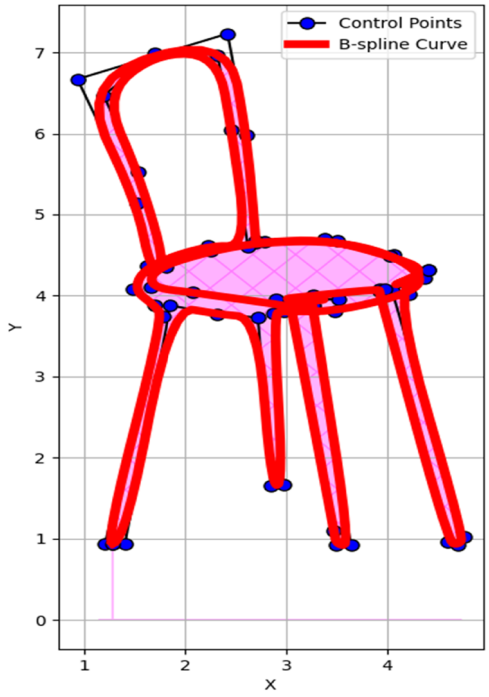

Figure 13: Shape of the plastic chair outline using the B-spline curve with control points [1.28, 0.94], [1.40, 0.94], [1.85, 3.88], [2.32, 3.77], [2.72, 3.73], [2.85, 1.65], [2.97, 1.67], [2.87, 3.78], [2.97, 3.81], [3.48, 3.80], [4.21, 4.02], [4.37, 4.22], [4.06, 4.50], [3.51, 4.67], [2.78, 4.66], [2.25, 4.55], [1.68, 4.33], [1.65, 4.10], [2.07, 4.04], [3.04, 3.87], [3.05, 3.85], [3.47, 1.10], [3.50, 0.92], [3.64, 0.92], [3.26, 3.87], [3.26, 3.88], [2.94, 3.90], [3.52, 3.96], [2.90, 3.95], [3.26, 4.00], [3.92, 4.08], [3.92, 4.05], [4.60, 0.96], [4.70, 0.92], [4.76, 1.02], [4.05, 4.05], [4.41, 4.31], [3.98, 4.08], [4.41, 4.31], [4.02, 4.49], [3.38, 4.70], [2.70, 4.65], [2.70, 4.67], [2.61, 5.98], [2.42, 7.23], [0.93, 6.67], [1.52, 5.14], [1.65, 4.31], [1.81, 4.35], [1.53, 5.52], [1.19, 6.47], [1.70, 6.99], [2.32, 6.97], [2.46, 6.05], [2.62, 4.60], [2.22, 4.62], [1.62, 4.37], [1.48, 4.08], [1.69, 3.88], [1.78, 3.74], [1.20, 0.93], and [1.28, 0.94].

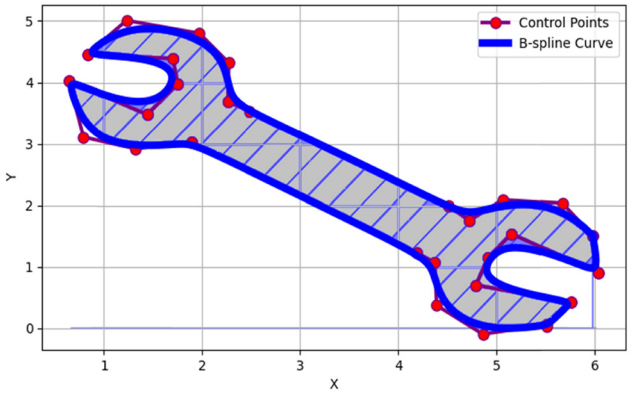

Figure 14: Shape of the wrench using the B-spline curve with control points [5.98,1.50], [5.67,2.03], [5.06,2.09], [4.72,1.76], [4.51,2.00], [2.48,3.54], [2.26,3.69], [2.27,4.32], [1.97,4.80], [1.23,5.01], [0.83,4.46], [0.83,4.46], [1.70,4.39], [1.75,3.98], [1.44,3.48], [0.64,4.03], [0.64,4.03], [0.79,3.11], [1.32,2.92], [1.89,3.02], [1.89,3.02], [4.19,1.23], [4.37,1.07], [4.39,0.37], [4.86,0.1], [5.51,0.06], [5.51,0.03], [5.76,0.42], [5.76,0.42], [4.79,0.70], [4.91,1.15], [5.15,1.54], [6.03,0.90], [6.03,0.90], and [5.98,1.50].

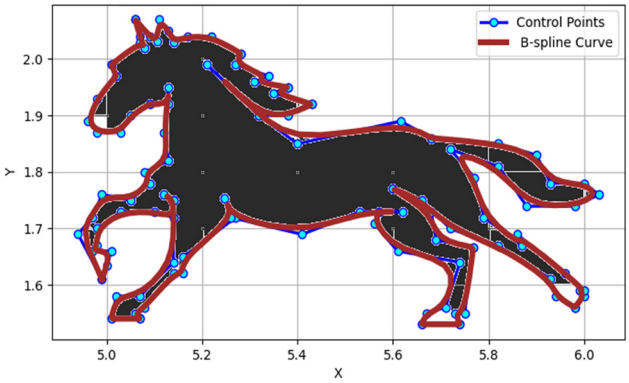

Figure 15: Horse outline using the B-spline curve with control points, including [4.99, 1.61], [5.00, 1.634], [5.01, 1.66], [4.97, 1.66], [4.98, 1.67], [4.98, 1.70], [5.03, 1.73], [5.10, 1.73], [5.14, 1.72], [5.14, 1.75], [5.12, 1.76], [5.14, 1.75], [5.14, 1.72], [5.14, 1.64], [5.07, 1.58], [5.02, 1.58], [5.01, 1.54], [5.01, 1.54], [5.07, 1.54], [5.07, 1.54], [5.06, 1.55], [5.08, 1.56], [5.14, 1.62], [5.16, 1.62], [5.16, 1.65], [5.27, 1.72], [5.247, 1.753], [5.26, 1.72], [5.41, 1.69], [5.53, 1.73], [5.62, 1.73], [5.57, 1.73], [5.57, 1.73], [5.56, 1.71], [5.61, 1.66], [5.74, 1.64], [5.71, 1.56], [5.67, 1.55], [5.66, 1.53], [5.66, 1.53], [5.74, 1.53], [5.74, 1.53], [5.73, 1.55], [5.75, 1.55], [5.768, 1.667], [5.768, 1.667], [5.69, 1.68], [5.68, 1.73], [5.60, 1.77], [5.60, 1.77], [5.66, 1.75], [5.72, 1.70], [5.82, 1.67], [5.93, 1.61], [5.94, 1.58], [5.98, 1.56], [5.98, 1.56], [6.00, 1.58], [5.99, 1.59], [6.00, 1.59], [5.96, 1.62], [5.86, 1.69], [5.87, 1.67], [5.79, 1.72], [5.77, 1.79], [5.72, 1.84], [5.82, 1.81], [5.88, 1.74], [5.98, 1.74], [6.03, 1.76], [6.00, 1.78], [5.93, 1.78], [5.90, 1.83], [5.82, 1.85], [5.68, 1.86], [5.68, 1.86], [5.616, 1.89], [5.4, 1.85], [5.32, 1.90], [5.21, 1.99], [5.32, 1.90], [5.38, 1.90], [5.43, 1.92], [5.43, 1.92], [5.35, 1.94], [5.38, 1.95], [5.38, 1.95], [5.31, 1.96], [5.34, 1.97], [5.27, 1.99], [5.28, 2.01], [5.28, 2.01], [5.22, 2.04], [5.17, 2.04], [5.14, 2.03], [5.13, 2.05], [5.11, 2.07], [5.106, 2.032], [5.09, 2.04], [5.06, 2.07], [5.06, 2.07], [5.07, 2.04], [5.08, 2.02], [5.07, 2.03], [5.01, 1.99], [5.01, 1.99], [5.02, 1.97], [5.02, 1.97], [4.98, 1.93], [4.96, 1.89], [4.98, 1.87], [5.03, 1.87], [5.05, 1.90], [5.09, 1.92], [5.09, 1.92], [5.13, 1.92], [5.13, 1.95], [5.12, 1.87], [5.13, 1.82], [5.08, 1.80], [5.09, 1.78], [5.05, 1.75], [4.99, 1.76], [4.97, 1.72], [4.94, 1.69], and [4.99, 1.61].

geometric modeling in everyday objects. To manufacture a smooth plastic chair shaped curve, we employed a second-degree B-spline along with non-uniform knot vectors comprising 65 knot values. Through the implementation of the de Boor algorithm with B-spline curves, we effectively developed both the initial chair shape and a refined, more polished rendition, exemplified in Figure 13.

5.5 Wrench designing

B-spline curves offer significant advantages in the design of wrenches, particularly in accuracy, longevity, and user comfort. Their ability to accurately represent complex shapes ensures that the wrench meets its specifications for effective performance. The smooth transitions and continuous forms created with B-splines enhance the durability by minimizing stress concentrations and manufacturing errors. Furthermore, the

flexibility in shaping allows for ergonomic designs, making the tool comfortable and functional for various hand sizes and grips. To create a smooth wrench shape, we utilized a fourth-degree B-spline curve with non-uniform knot vectors consisting of 40 knot values. Employing the de Boor algorithm alongside B-spline curves, we successfully crafted both the original wrench shape and an enhanced, refined version, as shown in the illustration provided in Figure 14.

5.6 Horse body outline

In horse body design, B-spline curves offer (Figure 15):

- ✓ Precision: local control allows for fine-tuning specific areas without altering the entire design.
- ✓ Durability: smooth transitions reduce the sharp edges, enhancing structural integrity and wear resistance.
- ✓ Ergonomics: continuous, natural curves match the horse's form, improving comfort and fit for better ergonomic design.

6 Conclusions

In conclusion, this article has offered an in-depth exploration of B-spline curves, examining their construction, properties, and real-world applications. Beginning with the mathematical foundations, we discussed the essential components that define B-spline curves' knot vectors, control points, basis functions, and degree, highlighting how these elements work together to create curves that are both smooth and versatile. The analysis detailed how the choice of knot vectors and the arrangement of control points provide precise local control over the shape of the curve, making B-spline curves a powerful tool for designers and engineers who require flexibility and accuracy. We also explored the intrinsic properties of B-spline curves, such as their local control property, convexity, continuity, and ability to handle complex geometries with minimal computational cost. By applying these properties, B-spline curves offer significant advantages in maintaining smooth transitions, optimizing curve fitting, and reducing unwanted oscillations, thereby achieving esthetically pleasing and functionally superior designs.

The practical applications discussed in this article showcase the broad utility of B-spline curves across various fields. We constructed a series of examples using these curves. These examples range from the aerodynamic contours of automobiles and the ergonomic shapes of electric irons and chairs to the intricate outlines of ceiling fans, wrenches, and character animations. They illustrate how B-spline curves can be manipulated through control points and the de Boor algorithm. This manipulation helps achieve desired shapes and functionalities, enhancing both visual appeal and ergonomic efficiency.

Furthermore, the exceptional smoothness and adaptability of B-spline curves provide a solid foundation for their future utilization in innovative applications. Their potential to improve the visual appeal and ergonomic design of various products remains a promising avenue for further exploration. As technology continues to advance, integrating B-spline curves into diverse fields such as architecture, biomedical engineering, and multimedia design holds the promise of creating more visually appealing and user-friendly products.

In essence, the exploration of B-spline curves offers a comprehensive overview of their theory and application. It also underscores their transformative role in shaping the future of design and engineering. Looking ahead, the potential of B-spline curves extends far beyond current applications. As technology progresses, their use is expected to expand into even more innovative domains. For instance, in adaptive architecture, B-spline curves could help create structures that respond dynamically to environmental changes. In biomedical engineering, they could assist in designing patient-specific implants and prosthetics with optimized forms and functions. Additionally, integrating B-spline curves into digital manufacturing and 3D printing processes could revolutionize the production of complex parts. This would lead to enhanced precision and reduced material waste.

Acknowledgment: The authors sincerely appreciate the valuable comments and suggestions provided by the anonymous reviewers, which have greatly contributed to improving the article.

Funding information: This work has not received any external funding.

Author contributions: All authors have accepted responsibility for the entire content of this manuscript and consented to its submission to the journal, reviewed all the results, and approved the final version of the manuscript. Md. N.A. and C.T.: visualization, validation, supervision, software, resources, project administration, methodology, investigation. N.M.: formal analysis, data curation, conceptualization. Md. F.A.A. and Md. S.H.: writing – review and editing, writing – original draft, visualization, validation, software, resources, formal analysis, data curation.

Conflict of interest: The listed authors have authorized the submission of their manuscript. and the authors declare no conflicts of interest. Furthermore, we confirm that this research has not received any external funding or financial support.

Data availability statement: No data were used for the research described in the article.

References

[1] Farin GE, Farin G. Curves and surfaces for CAGD: A practical guide. Elsevier Science; 2002.
[2] Laplace PS. Theorie analytique des probabilités. 3rd edn. Paris: Courcier; 1820.
[3] Chakalov L. On a certain presentation of the Newton divided differences in interpolation theory and its applications. Godishnik na Sofijskiya Universitet, Fiziko-Matematicheski Fakultet. 1938;34:353–94.
[4] Popoviciu T. Sur quelques propriétés des fonctions d'une ou de deux variables réelles. Ph.D. thesis. Cluj, Romania: Presented to the Faculte des Sciences de Paris, Published by Institutul de Arte Grafice Ardealul; 1933.
[5] Schoenberg IJ. Contributions to the problem of approximation of equidistant data by analytic functions. Part A–On the problem of smoothing or graduation. A first class of analytic approximation formulae. Quart Appl Math. 1946;4:45–99.
[6] Curry HB, Schoenberg IJ. On Polya frequency functions IV: The fundamental spline functions and their limits. J Anal Math. 1966;17:71–107.
[7] de Boor. On calculating with B-splines. J Approx Theory. 1972;6(1):50–62.
[8] Cox M. The numerical evaluation of B-splines. Inst Math Appl. 1972;10(2):134–49.
[9] Gordon WJ, Riesenfeld RF. B-spline curves and surfaces. Comput Aided Geom Des. 1974;23:91–126.
[10] Nascimbene R. An arbitrary cross section, locking free shear-flexible curved beam finite element. Int J Comput Methods Eng Sci Mech. 2013;14(2):90–103. doi: 10.1080/15502287.2012.698706.
[11] Gentilini C, Nascimbene R, Ubertini F. Towards an alternative approach to geometrical modelling of shell surfaces using a parametric representation. In: Computational fluid and solid mechanics 2003. Amsterdam: Elsevier Science Ltd; 2003. p. 288–91.
[12] Iqbal MK, Abbas M, Wasim I. New cubic B-spline approximation for solving third order Emden–Flower type equations. Appl Math Comput. 2018;331:319–33.
[13] Iqbal MK, Abbas M, Nazir T, Ali N. Application of new quintic polynomial B-spline approximation for numerical investigation of Kuramoto–Sivashinsky equation. Adv Differ Equ. 2020;2020:1–21.
[14] Iqbal MK, Abbas M, Zafar B. New quartic B-spline approximations for numerical solution of fourth order singular boundary value problems. Punjab Univ J Math. 2020;52(3):47–63.
[15] Iqbal MK, Abbas M, Zafar B. New quartic B-spline approximation for numerical solution of third order singular boundary value problems. Punjab Univ J Math. 2019;51(5):43–59.
[16] Park JH, Lee JW. Utilizing B-spline curves in architectural design: A case study of sustainable building facades. Sustain Archit Rev. 2019;12(3):87–95.
[17] Chang CH, Chen YH. Application of B-spline curves in industrial design. J Ind Des. 2017;25(2):45–54.
[18] Wang L, Zhang H. Application of B-spline curves in medical image reconstruction. J Med Imaging. 2020;35(4):156–63.
[19] Tan MK, Lim SH. Integration of B-spline curves in computer-aided manufacturing for precision engineering. Int J Precis Eng Manuf. 2018;19(6):1223–31.
[20] Rabah AB, Momani S, Arqub OA. The B-spline collocation method for solving conformable initial value problems of non-singular and singular types. Alex Eng J. 2022;61(2):963–74.
[21] Tayebi S, Momani S, Arqub OA. The cubic B-spline interpolation method for numerical point solutions of conformable boundary value problems. Alex Eng J. 2022;61(2):1519–28.
[22] Arqub OA, Tayebi S, Baleanu D, Osman MS, Mahmoud W, Alsulami H. A numerical combined algorithm in cubic B-spline method and finite difference technique for the time-fractional nonlinear diffusion wave equation with reaction and damping terms. Results Phys. 2022;41:105912.
[23] Wang F, Sohail A, Tang Q, Li Z. Impact of fractals emerging from the fitness activities on the retail of smart wearable devices. Fractals. 2024;32(1):2240112.
[24] Yu Z, Sohail A, Jamil M, Beg OA, Tavares JMR. Hybrid algorithm for the classification of fractal designs and images. Fractals. 2023;31(10):2340003.
[25] Tahir M, Ali S, Sohail A, Zhang Y, Jin X. Unlocking online insights: LSTM exploration and transfer learning prospects. Ann Data Sci. 2024;11(4):1421–34.
[26] Huang H, Shaheen S, Kottakkaran SN, Arain MB. Thermal and concentration analysis of two immiscible fluids flowing due to ciliary beating. Ain Shams Eng J. 2024;15(1):102278. doi: 10.1016/j.asej.2023.102278.
[27] Li Y, Leng Y, Baazaoui N, Arain MB, Ijaz N, Hassan AM. Exploring the dynamics of active swimmers microorganisms with electromagnetically conducting stretching through endothermic heat generation/assimilation flow: Observational and computational study. Case Stud Therm Eng. 2023;51:103560. doi: 10.1016/j.csite.2023.103560.
[28] Shaheen S, Huang H, Arain MB, Al-Zubaidi A, Tag-eldin EM. Concentration and thermal analysis of immiscible tangent hyperbolic fluid with distinct viscosity through horizontal asymmetric channel: Theoretical and observational study. Case Stud Therm Eng. 2023;50:103386. doi: 10.1016/j.csite.2023.103386.
[29] He Z, Usman AMB, Khan WA, Alzahrani AR, Muhammad T, Hendy AS, et al. Theoretical exploration of heat transport in a stagnant power-law fluid flow over a stretching spinning porous disk filled with homogeneous-heterogeneous chemical reactions. Case Stud Therm Eng. 2023;50:103406. doi: 10.1016/j.csite.2023.103406.
[30] Sun S, Li S, Shaheen S, Usman MBA, Khan KA. A numerical investigation of bio-convective electrically conducting water-based nanofluid flow on the porous plate with variable wall temperature. Numer Heat Transf Part A: Appl. 2023;2023:1–15. doi: 10.1080/10407782.2023.2242579.
[31] Arain MB, Zeeshan A, Alhodaly MSh, Fasheng L, Bhatti MM. Bioconvection nanofluid flow through vertical rigid parallel plates with the application of Arrhenius kinetics: A numerical study. Waves Random Complex Media. 2022;2022:1–18. doi: 10.1080/17455030.2022.2123115.

[32] Abu AO, Tayebi S, Baleanu D, Osman MS, Mahmoud W, Alsulami H. A numerical combined algorithm in cubic B-spline method and finite difference technique for the time-fractional nonlinear diffusion wave equation with reaction and damping terms. Results Phys. 2022;41:105912. doi: 10.1016/j.rinp.2022.105912.

[33] Tayebi S, Momani S, Abu Arqub O. The cubic B-spline interpolation method for numerical point solutions of conformable boundary value problems. Alex Eng J. 2022;61(2):1519–28. doi: 10.1016/j.aej.2021.06.057.

[34] Rabah AB, Momani S, Abu Arqub O. The B-spline collocation method for solving conformable initial value problems of non-singular and singular types. Alex Eng J. 2022;61(2):963–74. doi: 10.1016/j.aej.2021.06.011.

[35] Ni Q, Wang X. Shape analysis by computing geodesics on a manifold via cubic B-splines. Commun Math Stat. 2023;11:1–16. doi: 10.1007/s40304-023-00373-3.

[36] Lyche T, Manni C, Speleers H. Foundations of spline theory: B-splines, spline approximation, and hierarchical refinement. In: Lyche T, Manni C, Speleers H, editors. Splines and PDEs: From approximation theory to numerical linear algebra. Lecture notes in mathematics. Vol. 2219. Cham: Springer; 2018. p. 1–76. doi: 10.1007/978-3-319-94911-6_1.

[37] Alam MN, Li X. Non-uniform doo-sabin subdivision surface via eigen polygon. J Syst Sci Complex. 2021;34:3–20. doi: 10.1007/s11424-020-9264-z.

[38] Rogers DF, Adams JA. Mathematical elements for computer graphics. New York, NY: McGraw-Hill; 1990.

[39] Piegl LA, Tiller W. The NURBS book. Springer Berlin, Heidelberg; 2012.

[40] Hoschek J, Lasser D. Fundamentals of computer-aided geometric design. A K Peters/CRC Press; 2013.

[41] Schumaker LL. Spline functions: Basic theory. John Wiley and Sons; 2007.